Supplemental note: Case Reports

Family 1 (promoter/5'-UTR deletion)

The family comprises two affected children (the male proband III-4 and his elder sister III-1), both with syndromic craniosynostosis, who were born in the UK to first cousin parents of Pakistani origin. The pedigree is shown in Supplemental Fig 1. There was no additional family history of craniosynostosis and the parents (II-1 and II-2) were clinically normal. A history of 7 miscarriages in the mother II-2 was thought to be caused by antiphospholipid antibody syndrome (APS). A healthy sister III-2 was examined by a clinical geneticist and confirmed as unaffected. A boy III-3 was born at 29 weeks' gestation and died aged 1 month (mo), however further details about the cause of his death are not available.

During the pregnancy of the proband III-4, his mother was on anticoagulant therapy with heparin for the management of APS. He was born at 36 weeks' gestation by a caesarean section. The birth weight was 2.31 kg (-0.07 SD) and occipito-frontal circumference (OFC) was 35.6 cm (2.75 SD). At birth he exhibited asymmetry of the skull, prominent eyes, pointed long great toes and normal hands. A computed tomography (CT) scan at the age of 1 mo showed dilated ventricles without apparent obstruction, enlarged cerebrospinal fluid (CSF) spaces, cerebellar vermis hypoplasia and right coronal synostosis. He underwent a fronto-orbital advancement at the age of 1 year (yr). A small secundum atrial septal defect (ASD), another small (5 mm) ASD at the base of the ostium primum and a small (1 mm) patent foramen ovale (PFO) were detected at the age of 2 yr; there was minimal left to right shunt and management was conservative. At the age of 3 yr, he underwent bilateral cryptorchidism repair.

His development was moderately delayed. He was late in smiling, sat independently at the age of 1 yr, crawled at the age of 2 yr and was independently walking at the age of 2.5 yr. He had mild to moderate speech delay, which required speech therapy by the age of 5 yr. At primary school, he required extra support for literacy. His OFC was 49 cm (-2.1 SD) at the age of 6.5 yr. By the age of 8yr, he had been fitted with bilateral hearing aids because of conductive hearing loss, and had recurrent epistaxes of unknown cause. He was transferred to a school for special educational needs for his secondary education; at the age of 14 yr he continues to require help with his activities of daily living.

He had difficulties in eating and required pureed nutrients. His poor weight gain has been a persisting concern since the age of 3 years. At the age of 8 yr, he was diagnosed with iron deficiency anemia. His feeding difficulties persisted, aged 14 yr he had entered puberty, his height was 149.5 cm (-1.72 SD) and weight was 24.6 kg (-4.4 SD); he was able to eat only small amounts and was receiving most of his nutrition by liquid feed via nasogastric tube and pump.

He felt full early when feeding orally or by nasogastric tube, and had the urge to vomit if volumes were increased. In addition he was noted to be developing a scoliosis (20°); he had hypospadias and his fingers appeared relatively long. He has episodes of sleep apnea of unknown cause.

Genetic investigation revealed a heterozygous 200 kb deletion at 22q12.3 involving *LARGE1* (HGNC:6511) on chromosomal microarray; this deletion was also identified in the unaffected father, so was considered likely to be non-pathogenic.

The proband's elder sister III-1 was born at 35 weeks' gestation by a caesarean section owing to poor indices on Doppler monitoring. The mother was also on anticoagulant therapy for this pregnancy. The birth weight was 2.04 kg (-0.45 SD). Brachycephaly and ASD were diagnosed on day one of life. A CT scan at the age of 1 yr showed bicoronal synostosis, possible left lambdoid synostosis and fused anterior skull base, but no brain abnormality. Clinically, she had a slightly hooked nose, a high palate and watering eyes. Her hands and feet were small with normal digits and a normal motion range of the joints. She was diagnosed as having Crouzon syndrome and underwent a fronto-orbital advancement at the age of 2 yr. By the age of 8 yr, she had developed a class III malocclusion with midfacial hypoplasia. The ASD was closed using a catheter procedure (with Amplatzer device) by the age of 10 yr. At 10 yr of age, she was diagnosed with scoliosis, which required a brace treatment and posterior instrumented correction at 12 yr. She was also diagnosed with psoriasis at the age of 12 yr. In addition she was noted to have vesicular milia-like lesions on either side of the nose and long fingers.

She was late in smiling and had a mild delay in motor development during infancy, sitting independently at 1 yr, crawling at 1 yr and independently walking after 2 yr. She had a mild to moderate speech delay which required speech therapy and temporary hearing aids, but hearing loss was thought to be caused by glue ear. She attended normal school and had adapted to school well at the age of 15 yr. At the age of 21 years she is working at a call centre. She had difficulty in gaining weight; her weight and height at 12 yr were 23.1 kg (-3 SD and 134.4 cm (-2.2 SD), respectively.

Conventional genetic testing of craniosynostosis-related genes was performed for *FGFR3* (HGNC:3690) Pro250Arg, *FGFR2* (HGNC:3689) exon 8 and 10, and multiplex ligation-dependent probe amplification (MLPA) and sequencing for *TWIST1* (HGNC:12428), however, no causal variants were identified. Following enrolment in the *Genetic Basis of Craniofacial Malformations* study, exome sequencing (ES) was performed on a sample from III-4 and genome sequencing (GS) on III-1 (details in Supplemental Table 1). Segregation of variants was additionally tested in the unaffected sister III-2. The homozygous 4 kb deletion partly overlapping the 5' untranslated region (5'-UTR) of *DHRS3* (HGNC:17693) was uniquely consistent with the disease segregation in the sibship. The *DHRS3* gene

was registered in GeneMatcher,[1] leading to the identification of Families 2, 3 and 5 described below.

Family 2 [p.(Val110Ile)]

This family was previously published ("Family 9") as part of a series of consanguineous Jordanian families investigated for causes of intellectual disability.[2] Two girls (the proband III-2, and III-3) and their brother (III-4), the offspring of first cousin parents, presented with motor delay and intellectual disability; they had two cousins with similar phenotypes. The 16-year old proband demonstrated aggressive behavior. Exome sequencing of this individual initially identified 8 candidate variants (see Table 13 of ref. 2), of which the homozygous variant c.328G>A; p.(Val110Ile) in *DHRS3* was highlighted as potentially causative.

Following the original molecular and biochemical investigations of the family, contact was lost and no further clinical information is available.

Family 3 [p.(Val171Met)]

The 52-year-old female (II-2) was the second child of healthy non-consanguineous Spanish parents originating from the same village. Her first sister died soon after birth due to respiratory insufficiency. The patient has a younger brother (II-3) aged 46 yr without any relevant health issues to date.

During infancy, investigation for brachycephaly led to a diagnosis of unilateral left coronal craniosynostosis. Surgery was not performed. A clinical diagnosis of Crouzon syndrome was made at that time. A karyotype performed in infancy was normal.

Mild developmental delay was evident in infancy, although motor and language milestones were within the normal range. She presented mild learning difficulties needing support at school. No formal psychometric evaluation was performed. Mild scoliosis was diagnosed during adolescence, this was monitored by orthopedics and rehabilitation and did not require bracing or surgery. She finished secondary education and was working as administrative assistant. She always lived with her parents although she has autonomy for daily living activities.

Surgical repair of a right inguinal hernia was performed when she was 42 years old. At the age of 51 years she was found to be hypertensive and a systolic heart murmur was detected. Echocardiogram revealed aortic root dilatation which was thought to be associated with pseudocoarctation of the aorta. Bilateral conductive hearing impairment was also diagnosed, but this has not required hearing aids to date.

At the age of 52 years she was referred for a clinical genetics evaluation following the diagnosis of aortic root dilatation, because of suspected Turner syndrome. Her height was 157 cm (-0.95 SD), weight 57.4 kg (0 SD), OFC 52 cm (-2.2 SD); she was noted to have dysmorphic features including facial

asymmetry, proptosis, hypertelorism, low-set ears, high, narrow palate, broad neck and low posterior hairline.

Blood analyses, including metabolic and hormonal screening, gave normal results. Genetic testing comprised microarray, gene panel including genes related to Noonan syndrome, and ES (Supplemental Table 1). The bioinformatics pipeline in ES reanalysis, including OMIM genes not known to be associated with any genetic disease, allowed the identification of single nucleotide variants and small insertions and deletions after comparing to the reference human genome (NCBI v37 version). Variant filtering and prioritization revealed a homozygous missense variant, c.511G>A; p.(Val171Met) in *DHRS3*, as the only credible disease-causing candidate. The variant was present in heterozygous state in both parents and her healthy brother is homozygous wild type for this variant. The variant information was entered into GeneMatcher,[1] enabling the details to be linked up to previously identified cases in this series.

Family 4 [p.(Val171Met)]

The family comprises two affected siblings from Mexico (II-1 and II-2), the offspring of consanguineous parents. Both the affected male (II-1, aged 22 years) and his sister (II-2, aged 18 years) presented with facial dysmorphism (triangular face, mild proptosis, and hypoplastic midface), bilateral coronal craniosynostosis, thoraco-lumbar scoliosis, bilateral carpal fusions, moderate sensorineural hypoacusis and borderline intellectual functioning. In addition, II-1 was diagnosed with unilateral grade 1 microtia, and thenar and hypothenar hypoplasia; he had an atrial septal defect that was surgically repaired at the age of 9 years. II-2 presented with bilateral tarsal fusions and congenital anal fistula corrected with surgery.

Exome sequencing of both affected individuals was performed as summarized in Supplemental Table 1. Given the likely recessive inheritance, filtering was used to identify variants with minor allele frequency <0.01 in the gnomAD database v.2 (global and in the Americas) and present in both siblings in either homozygous or putatively compound heterozygous state. Gene mining and literature review highlighted a homozygous variant in *DHRS3* (c.511G>A; p.(Val171Met)), as the only candidate potentially associated with craniosynostosis. Analyses of known craniosynostosis-related genes including *FGFR1*, *-2*, and *-3* were negative.

Family 5 [p.(Glu244Gln)]

The male patient (III-1) is the first child of healthy parents originating from Syria but residing in Germany, who are related (first cousins). The family history is unremarkable. Prenatal ultrasound revealed a tentative diagnosis of premature craniosynostosis, the fetal karyotype was normal (46,XY).

The patient was born at term with normal measurements for weight and length, but macrocephaly [weight: 3420 g (-0.23 SD), length 52 cm (0.18 SDand OFC 39.5 cm (+2.23 SD)]. Clinical signs of frontonasal dysplasia with right cleft lip and palate and left cleft palate were noted; craniosynostosis was excluded. A tentative clinical diagnosis of frontonasal dysplasia type Guion-Almeida was proposed. The clefts were surgically corrected. An occipital meningocele was present, subsequently surgically removed, and brain magnetic resonance imaging (MRI) revealed agenesis of the corpus callosum, schizencephaly, absence of the cerebellar vermis and dysplastic cerebellar hemispheres. Ophthalmological examination revealed severely reduced vision, which was associated with nystagmus and divergent strabismus. Hearing was tested to be normal. He had seizures in the newborn period, these were successfully controlled with phenobarbital. Nasogastric tube feeding was necessary for several weeks. Chromosomal microarray demonstrated a duplication in 12q24.33, which was considered likely coincidental to the phenotype as it was maternally inherited.

Clinical examination was performed at the age of 3.5 years. Weight was 11.5 kg (-2.55 SD), height was 89 cm (-2.52 SD) and OFC was 52 cm (+0.88 SD). He was hypotonic, able to grasp objects and to turn onto his side from a supine position, but was unable to roll or crawl. He had no active speech. He showed marked facial dysmorphism with severe hypertelorism, downslanting palpebral fissures, low-set and posteriorly rotated ears; his fingers were tapering.

Exome sequencing data (Supplemental Table 1) were analysed using the Human Phenotype Ontology (HPO) terms Cleft lip, Cleft palate, Global developmental delay, Motor delay, and Cerebellar hypoplasia. Filtering for known variants in ClinVar and HGMD revealed the heterozygous variant NM_000257.4:c.2606G>A; p.(Arg869His) in *MYH7* (HGNC:7577), this was considered to be an additional finding unrelated to the clinical presentation. Three *de novo* missense variants (in *MUC4* [HGNC:7514], *NUTM2G* [HGNC:23449] and *VCX3A* [HGNC:18159]) arose in genes that have low gnomAD v2 missense Z-scores and were predicted benign by multiple criteria, hence were not considered pathogenic. Five homozygous missense variants were identified, in the genes *AHNAK* (HGNC:347), *ANK3* (HGNC:494), *DHRS3*, *MPZL2* (HGNC:3496) and *PC* (HGNC:8636), that have a MAF < 0.01 and do not occur in homozygous state in gnomAD; all have CADD scores >20, variable REVEL scores, but are predicted likely benign by AlphaMissense (Table S5). Variants in 3 of these 5 genes are classified in OMIM as being responsible for autosomal recessive disease genes (*ANK3* - Intellectual developmental disorder, autosomal recessive 3; *MPZL2* - Deafness, autosomal recessive 111; *PC* - Pyruvate carboxylase deficiency). However none of the specific variants has been described in the corresponding disease, and none of the diseases feature craniofacial malformations as present in the patient. Following contact through GeneMatcher,[1] we investigated the potential significance of the c.730G>C, p.(Glu244Gln) variant identified in *DHRS3*.

Supplemental Methods

Additional Molecular Biology Methods for Family 1

DNA extraction. DNA was extracted from whole blood samples collected into EDTA tubes, from lymphoblastoid cell lines, or from fibroblast cell lines established from scalp skin obtained during surgery. DNA was extracted using the Nucleon Blood and Cell Culture (BACC) DNA extraction kit (Gen-Probe Inc.), according to the manufacturer's protocol. Initial clinical genetic analysis for causes of craniosynostosis in individual III-1, including *FGFR2, FGFR3,* and *TWIST1*, did not provide a molecular diagnosis.

RNA extraction and cDNA synthesis. RNA from human samples was extracted from whole blood, Epstein–Barr virus (EBV)-transformed lymphoblastoid cell lines or fibroblast cell lines. Blood samples were collected into PAXgene Blood RNA tubes and the PAXgene Blood RNA Kit (PreAbalytiX) was used to extract the RNA. RNA was extracted from lymphoblastoid or fibroblast cell lines using Trizol reagent (Invitrogen) and the RNeasy kit (Qiagen). cDNA synthesis was performed with the RevertAid First Strand Synthesis kit (Thermo Fisher Scientific) using either oligo (dT) primers or random hexamer primers according to the manufacturer's instructions.

Polymerase chain reaction (PCR). Primers were designed using Primer3 web version 4.0.0.0 (http://primer3.ut.ee/) and it was confirmed that the primers did not overlay single nucleotide polymorphisms (SNPs) and were specific by using the University of California Santa Cruz (UCSC) In-Silico PCR program. Primer sequences are provided in Table S2.

PCR reactions were performed using FastStart Taq DNA Polymerase (Roche). The reaction was carried out using 20 ng of genomic DNA in a total volume of 20 µl, containing 2 µl of PCR reaction buffer (10x) with 20 mM $MgCl_2$, 1 µl of nucleotide mix (25 µM each dNTP), 1 µl each of 0.2 µM forward and reverse primers, 0.15 µl of FastStart Taq DNA Polymerase (5 U/µL) and H_2O. Cycling conditions consisted of an initial step of 5 min denaturation at 94˚C, followed by 35 cycles of 94˚C for 30 s, annealing at 63˚C for 30 s and extension at 72˚C for 30 s, and a final extension step at 72˚C for 7 min. For the multiplex PCR shown in Figure 2A, 1 µl each of three primers was used.

Screen for *DHRS3* variants in the craniosynostosis cohort. Universal CS1 (5'-ACACTGACGACATGGTTCTACA-3') and CS2 (5'- TACGGTAGCAGAGACTTGGTCT-3') adaptor sequences were added to the 5' end of all target-specific forward and reverse primers, respectively, for the barcoding PCR amplification. To enable multiplex PCR amplification, primers were combined and optimized to obtain a relatively equal intensity of bands from each product on a 3% agarose gel. Mixture of primer pairs comprising (A) exon 1-2 and exon 6 with 1:4 ratio, (B) exon 1-3, 2 and 3 with

1:1:1 ratio and (C) exon 1-1 and exons 4 and 5 with 8:1:1 ratio were optimal. Using these 3 primer mixes, 3 multiplex PCRs were performed with 20 ng of patient DNA using the KAPA Taq HotStart PCR kit (Kapa Biosystems) according to the manufacturer's protocol.

PCR products from each reaction were pooled and 1 µl of a 1 in 100 dilution of the total PCR pool was used for the barcoding PCR with the Access Array Barcode Library for Illumina Sequencers – 384 (SingleDirection) (Fluidigm, PN100-4876). The barcoding PCR was performed using Q5 High Fidelity DNA polymerase (QIAGEN) according to the manufacturer's protocol. The barcoded products were pooled and purified using AxyPrep MagPCR Clean-up kits (Appleton Woods) to produce libraries for sequencing on the MiSeq. Variant calling and coverage analysis data were obtained using the amplimap pipeline.[3]

Bioinformatic analysis of Genomics England 100,000 Genomes (100kGP) Rare Disease cohort

We extracted all variants in *DHRS3* that had been called in all rare disease participants (proband and family members) of the 100kGP. The output was filtered was by allele frequency (gnomAD less than 0.05), CADD score above 20, and protein-coding consequence, and homozygous variants were extracted from the list. In addition we screened remaining patients if they had two variants that conformed to the above criteria (ie potential compound heterozygous variants). Variants were visualized using the Integrative Genomics Viewer (IGV).[4]

Subpopulation stratification of retinoid measurements

The basis for stratification is supported by the Index of Individuality (Ii), which is a clinical concept that considers the within participant and between participant variability to determine the utility of a population-based reference value.[5,6] For population reference values to have utility in determining excess or deficiency from a single sample from an individual, the index of individuality should be >1.4.[5,6] Index of individuality for RA (0.86), ROL (0.27), and 13cRA (0.60) are all less than 1, indicating that population reference intervals are of limited utility for diagnosis of deficiency or excess.[7] In these cases where the within participant variation is much less than the between participant variation (i.e., a low Ii value), it is important to stratify populations and obtain separate reference intervals. [5-7] Additionally, in the case where no wild-type (WT) was available in the subpopulation, comparison to heterozygotes to establish the reference range is a valid concept to determine disease where the reference population may not be a healthy group (but is at steady-state).[6,8] Animal models support the observations in human in regards to unique subpopulations according to genetic and/or dietary environment, for example, in mouse models, retinoids varied by genetic (WT) strain and the amount of vitamin A in the diet in a strain specific manner.[9] A similar correlation was observed in the *Cynomolgus* nonhuman primate, in which plasma RA and 13cRA increased after either RE or ROL dosing in a dose-dependent manner.[10]

Here, we stratified each family into a unique subpopulation and calculated a notional reference interval defining the thresholds for excess or deficiency using the reported critical difference at the 95% confidence level and the average WT value, or heterozygous value if no WT was available.[7,11] Our results indicate the necessity for similarly sourced controls for patient evaluation with unaffected individuals from the same family as preferable, and individuals from the same geographic-nutritional environment being acceptable.

scRNA-seq analysis of gene expression in the retinoic acid (RA) signaling pathway

Data were extracted from https://www.facebase.org/chaise/record/#1/isa:dataset/RID=3TYP. E18.5 stage scRNA-seq datasets scWCE18_196.count and scWCE18_S198_matrix.count were analyzed. Cells with percentage mitochondria of greater than 5% and 20% were excluded from data scWCE18_S196 and scWCE18_S198, respectively. Cells with a Feature count of more than 800 and less than 7500 were further selected to filter out potentially unhealthy cells. Standard Seurat SCT into Integration workflow was performed using the new V2 regularization method, which led to the identification of 10 clusters at resolution=0.2 using the 30 top PCs. A second unsupervised clustering at resolution=0.5 was performed using the 25 top PCs on the coronal suture populations, which consist of clusters 0, 1, 2, 3 and 5. This analysis led to nine populations that correspond to the original paper (Holmes et al., 2021). Genes involved in retinoic acid synthesis, transport and degradation were subsequently assessed in the 9 distinct cell populations using Dotplot visualization in Seurat.

Skeletal preparation of mouse neonates

E14.5-17.5 embryos were stained with either Alcian blue, or both Alcian Blue and Alizarin red, for cartilage alone or cartilage and bone, respectively, using established procedures[12] with the following modifications. Pregnant dams were euthanized by CO_2 asphyxiation, and mouse embryos were collected into ice-cold phosphate-buffered saline (PBS) for approximately 30-40 min to induce anesthesia by hypothermia, before being fixed in ice-cold 95% ethanol. Skin and abdominal organs were removed after which the embryos were equilibrated in base solution (70% ethanol, 5% acetic acid), and then stained overnight in fresh staining solution (70% ethanol, 5% acetic acid, 0.02% Alcian blue, 0.005% Alizarin red). The next day, the embryos were briefly rinsed in base solution, then in water, followed by 2% potassium hydroxide (KOH) to digest soft tissues. After sufficient soft tissue digestion (~ 3-4 hr for E14.5 embryos and 5-6 hr for E17.5 embryos), embryos were rinsed in 0.25% KOH for 30 min and then cleared in an ascending KOH-glycerol series (0.25% KOH-10% glycerol, 0.25% KOH-20% glycerol, 0.25% KOH-30% glycerol) before storing long-term in 50% and then 100% glycerol.

β-galactosidase (LacZ) Staining

RARE-lacZ mice were a generous gift from Janet Rossant and were maintained and genotyped as previously described,[13] in accordance with the Stowers Institute for Medical Research IACUC approved protocol 2022-143. E18.5 mouse embryos were dissected, and the heads were isolated and fixed in 0.2% glutalaldehyde/2% formalin in PBS for 1.5 hr at 4 ^{o}C. The embryos were then washed 3 x 15 min in cold PBS, and immersed in prewarmed X-gal staining solution (5 mM potassium ferricyanide, 5 mM potassium ferrocyanide, 2 mM $MgCl_2$, 0.01% sodium deoxycholate, 0.02% Nonidet P-40). After adding 40 mg/ml X-gal the embryos were incubated at 37 ^{o}C overnight with rocking.

Supplemental Results: Plasma Retinoid Profile

Retinol (ROL; vitamin A). As DHRS3 catalyzes the reduction of retinaldehyde (RAL) to ROL, plasma ROL was quantified to assess the DHRS3 variants. Figure 5A shows that homozygotes have lower levels of plasma ROL compared to WT (Family 1 [5'-UTR deletion], Family 3 [p.(Val171Met)]). Some specific comparisons include: Family 1 - Hom (III-1 and III-4) and Het family members (II-2 and III-2) have significantly decreased plasma ROL compared to unrelated WT controls (C1, C2); note that Hom (III-1) from Family 1 has significantly less plasma ROL than WT and is below the threshold for vitamin A deficiency (0.7 nmol/mL). Hom (III-4) has significantly less plasma ROL than WT and is considered to be low vitamin A status (0.7-1.05 nmol/mL).[14] Family 2 - Hom (III-2) has decreased plasma ROL compared to unaffected Het family members (II-2 and III-5); notably, all heterozygotes and homozygotes are of low vitamin A status (0.7-1.05 nmol/mL) with Hom (III-2) below the threshold for vitamin A deficiency. Family 3 - Hom (II-2) has significantly decreased plasma ROL compared to her WT sibling (II-3) and unrelated controls (C3, C4); note that plasma ROL of the Hom (II-2) is also considered to be low vitamin A status. Family 5 - Hom (II-1) and Het parent (I-2) have significantly reduced plasma ROL compared to Het parent (I-1); the Het (I-2) shows plasma ROL levels similar to the Hom (II-1). In some cases, heterozygous individuals have similar ROL levels to homozygotes, where DHRS3 loss of function may be exacerbated by low nutritional input (Family 1 [5'-UTR deletion], Family 2 [p.(Val110Ile)], and Family 5 [p.(Glu244Gln)]). These data showing reduced plasma ROL are consistent with diminished catalytic activity of DHRS3. It should be noted that ROL, as the substrate for RA biosynthesis, is typically 100-1000x greater in abundance than its active metabolite RA.[15] Even at the most reduced plasma ROL levels observed here, plasma ROL is present at 100x greater levels than RA indicating there is still ample substrate for RA synthesis.

Endogenous RA isomers. For completeness, we provide the data for other endogenously occurring isomers of RA in human plasma (Figure S6, S7, S8). In addition to RA (all-*trans* RA), there are several other isomers detected in human plasma: 13-cis RA (13cRA), 9-cis RA (9cRA), and 9,13-di-cis RA (9,13dcRA). In this study, we observed a similar endogenous isomer distribution as has been reported by us and others for RA in human plasma.[16-18] It should be noted that the analytical method used to quantify RA has been thoroughly validated[15,18-20] and applied in over 50 publications. The analytical variation of the method is ~4%. The analytical method for ROL and RE has similar variation and has been similarly validated and applied.[15,21] The absence of batch effects was confirmed by reanalysis of selected samples, for which values were obtained that were similar to the initial analysis and are included as individual points on the respective retinoid graphs (Figure 5, S6 to S9).

RA is the main active metabolite in plasma. In all four families, plasma levels of RA in the homozygous individuals were significantly higher than in heterozygous or WT individuals from the

same family, or in unaffected controls obtained and processed simultaneously to the family (Figure 5B). This indicates that all four variants analyzed are functionally significant and diminish the catalytic activity of DHRS3, consistent with variant computational modeling. Some specific comparisons include: Family 1- Hom (III-1 and III-4) have significantly increased plasma RA compared to both unaffected Het family members (II-2 and III-2) and unrelated WT controls (C1, C2); Family 2 - Hom (III-2, III-3, and III-4) all have elevated plasma RA compared to unaffected Het family members (II-2 and III-5), except III-2 versus III-5; Family 3 - Hom (II-2) has significantly elevated plasma RA compared to WT sibling (II-3) and unrelated controls (C3, C4); Family 5 - Hom (II-1) has significantly elevated plasma RA compared to Het parents (I-1 and I-2).

13cRA has low affinity for retinoic acid receptors (RARs) and is considered biologically inactive. 13cRA was similar in trends to RA, except for Family 1 (5'-UTR deletion), in which homozygous and heterozygous individuals had lower 13cRA than WT. Family 2 (p.(Val110Ile)), Family 3 (p.(Val171Met)), and Family 5 (p.(Glu244Gln)) exhibited higher levels of plasma 13cRA in homozygous compared to WT or heterozygous individuals (Figure S6). Some specific comparisons include: Family 1 - Hom (III-4) and Het (II-2) have significantly decreased plasma 13cRA compared to unrelated WT controls (C1, C2); Family 2 - Hom (III-2, III-3, and III-4) and Het (III-5) all have elevated plasma 13cRA compared to the unaffected Het family member II-2; Family 3 - Hom (II-2) has significantly elevated plasma 13cRA compared to her WT sibling (II-3) and unrelated controls (C3, C4); Family 5 - Hom (II-1) has significantly elevated plasma 13cRA compared to his Het parents (I-1 and I-2). The plasma 13cRA being higher in WT controls for Family 1 (5'-UTR deletion) compared to controls in Family 2 (p.(Val110Ile)), Family 3 (p.(Val171Met)), or Family 5 (p.(Glu244Gln)) is consistent with distinct retinoid profiles according to dietary vitamin A. As previously documented,[22] higher quantities of 13cRA were quantified in plasma when participants were dosed with retinyl palmitate (preformed vitamin A), whereby the increase from baseline for 13cRA was proportionally greater compared to the increase in RA, which is consistent with our measured values - 13cRA is comparatively higher in Family 1 vs. Families 2, 3, & 5 (171-820%) compared to RA in Family 1 vs. Families 2, 3, & 5 (46-125%).

9cRA is a high affinity ligand for both RARs and retinoid X receptors (RXRs), however its measured concentrations are limited in location and amount. In plasma, levels are typically 10-100x lower than RA.[17,18] Plasma 9cRA was higher in homozygous, compared to WT or heterozygous individuals in Family 1 (5'-UTR deletion), Family 2 (p.(Val110Ile)), Family 3 (p.(Val171Met)), and Family 5 (p.(Glu244Gln)) (Figure S7). Some specific comparisons include: Family 1 - Hom (III-1 and III-4) have significantly increased plasma 9cRA compared to unrelated WT controls (C1, C2); Family 2 - Hom (III-2) has elevated plasma 9cRA compared to unaffected Het family members (II-2 and III-5);

Family 3 - Hom (II-2) has significantly elevated plasma 9cRA compared to her WT sibling (II-3) and unrelated controls (C3, C4); Family 5 - Hom (II-1) has significantly elevated plasma 9cRA compared to his Het parents (I-1 and I-2). Here, measured plasma levels of 9cRA were 8-69x lower than RA (Figure 5B, S7). 9cRA excess produces developmental malformations similar to equal concentrations of RA.[16,23,24]

9,13dcRA has low affinity for RAR and is considered biologically inactive. 9,13dcRA can vary during pregnancy and increase after dosing with 9cRA.[16] Plasma 9,13dcRA was higher in homozygous compared to WT or heterozygous individuals in Family 1 (5'-UTR deletion), Family 3 (p.(Val171Met)), and Family 5 (p.(Glu244Gln)); Family 2 (p.(Val110Ile)) had similar levels in homozygous and heterozygous individuals (Figure S8). Some specific comparisons include: Family 1 - Hom (III-1) has significantly increased plasma 9,13dcRA compared to unrelated WT controls (C1, C2); Family 2 - individuals have similar 9,13dcRA levels; Family 3 - Hom (II-2) has significantly elevated plasma 9,13dcRA compared to her WT sibling (II-3) and unrelated controls (C3, C4); Family 5 - Hom (II-1) has significantly elevated plasma 9,13dcRA compared to his Het parents (I-1 and I-2).

Retinyl ester (RE). RE is the esterified form of ROL. Of note, plasma samples in this study were not collected after fasting. Traditional population ranges for RE are from the fasting state.[25-27] Plasma levels of RA, RA isomers (13cRA, 9cRA, 9,13dcRA), and ROL are not affected by food intake,[17,22] however postprandial RE varies significantly.[25,26,28,29] Our measured values (Figure S9) are similar to those previously reported for postprandial measurements of RE in plasma.[26,28] Because the RE levels are not from the fasted state and have a variable post-prandial effect, no interpretation with regard to genotype should be made. However, for illustrative purposes, the critical difference for ROL was used as a surrogate to indicate likely reference ranges. According to variant, Family 1 (5'-UTR deletion) had significantly lower plasma RE levels in homozygous and heterozygous individuals compared to WT, whereas Family 2 (p.(Val110Ile)) and Family 3 (p.(Val171Met)) had levels that were unchanged and/or variable. Some specific comparisons include: Family 1 - Hom (III-1 and III-4) and Het family members (II-2 and III-2) have significantly decreased plasma RE compared unrelated WT controls (C1, C2); Family 2 - individuals have similar plasma RE levels; Family 3 - individuals have similar plasma RE levels; Family 5 - Hom (II-1) has significantly increased plasma RE compared to his Het parents (I-1 and I-2). Importantly, fasting plasma samples would be needed to determine the effect of *DHRS3* variants on plasma RE.

In vitro Cellular Retinoid Profile

DHRS3 reduces RAL to ROL and limits the production of RA. ROL, as the end-product of DHRS3 enzymatic activity, and RA, as the tightly controlled active metabolite of vitamin A, were quantified as indicators of DHRS3 enzymatic activity. These in vitro data showing reduced ROL and increased RA

are consistent with diminished catalytic activity of DHRS3, both after treatment with substrate RAL and at basal levels. Trends in the levels of ROL are rarely directly proportional to the trends in its active metabolite RA, which is typically present at 100-1000x lower abundance than ROL.[15] It should be noted that RA is a potent transcriptional regulator and changes in its concentration are functionally amplified through physiological signaling mechanisms, in contrast to the ROL substrate.

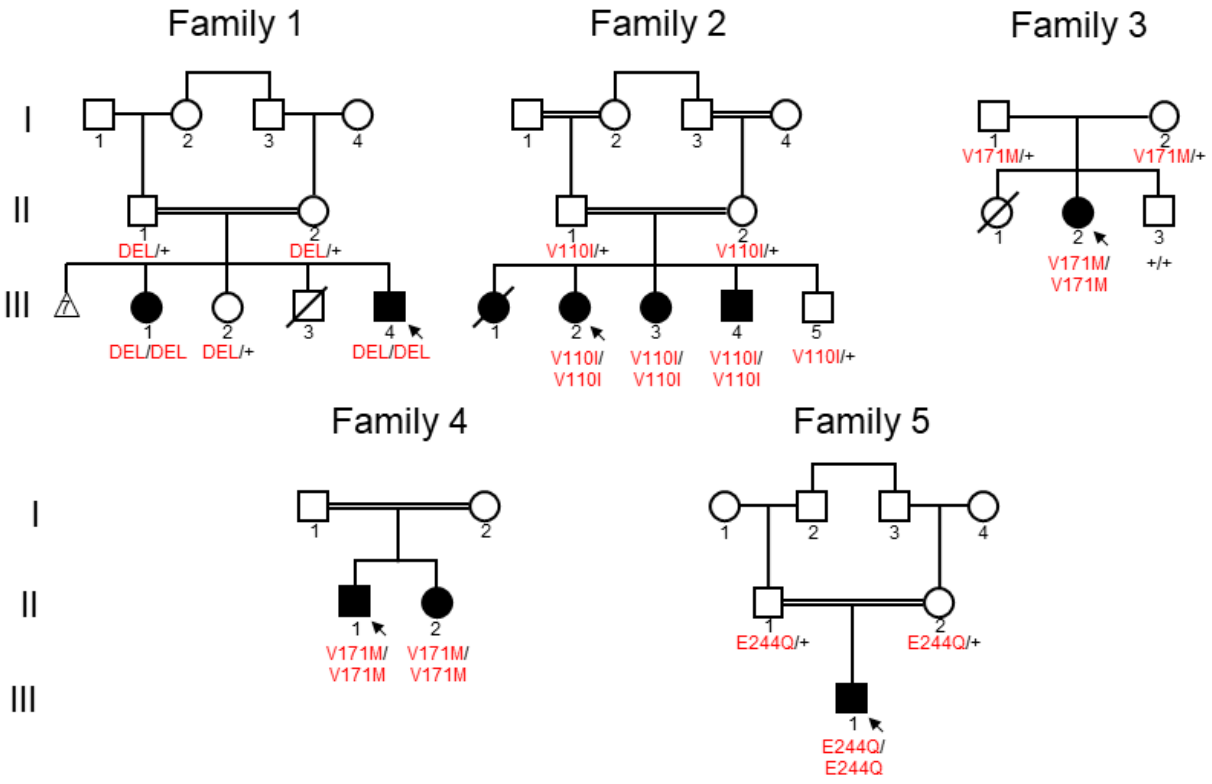

Supplemental Fig 1. Pedigrees and genotyping of families segregating *DHRS3* homozygous variants.

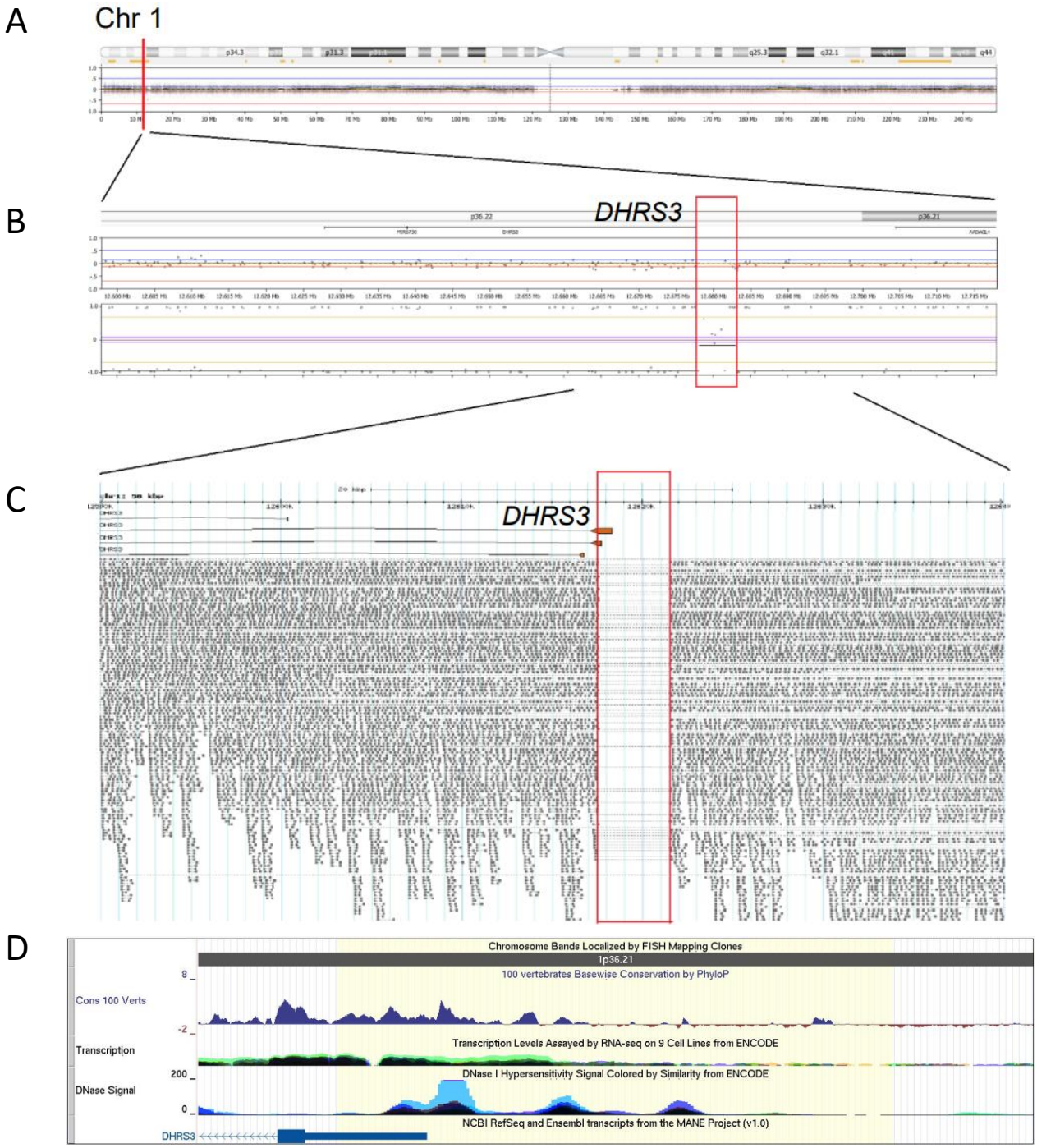

Supplemental Fig 2. Identification of homozygous deletion of *DHRS3* promoter and 5'-UTR in individual III-1 from Family 1.

(A) Illumina Infinium Omini2.5 Exome v1.2 SNP chip analysis, screenshot view of chromosome 1. Horizontal yellow lines immediately under the chromosome ideogram indicate loss of heterozygosity regions. Vertical red line shows the location of the deletion. (B) Expansion from the top panel of the deleted region, the red rectangle encloses the deletion called by Nexus Copy Number software. Ten consecutive points are missing in the panel of Log R Ratio (top). B allele frequency (bottom) shows random plots in the region of the deletion. (C) GS analysis of III-1, visualized in GBrowse.[30] *DHRS3* exon 1 is shown in brown blocks in the middle. Black marks indicate the individual read pairs mapped to the genome. Red rectangle shows the region of homozygous deletion in the patient; note multiple read pairs spanning the deleted region (joined by dotted lines). (D) UCSC Genome Browser (GRCh38) visualization of the deleted region (pale yellow). Additional tracks show 100 vertebrate conservation, ENCODE RNASeq and DNAse 1 hypersensitivity.

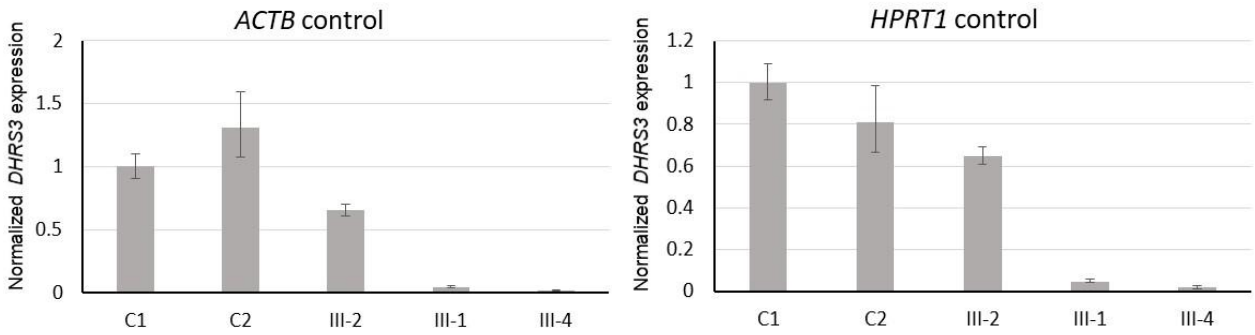

Supplemental Fig 3. **Expression of *DHRS3* in lymphoblastoid cell lines of individuals from Family 1 (promoter/5'-UTR deletion).**

Results are shown for two control samples (C1, C2), a heterozygote for the deletion (III-2), and the two homozygous affected children (III-1 and III-4). Results are plotted as mean ± standard deviation of 3 biological replicates, normalized to either *ACTB* (left) or *HPRT1* (right) expression and relativized to the mean value of the C1 sample.

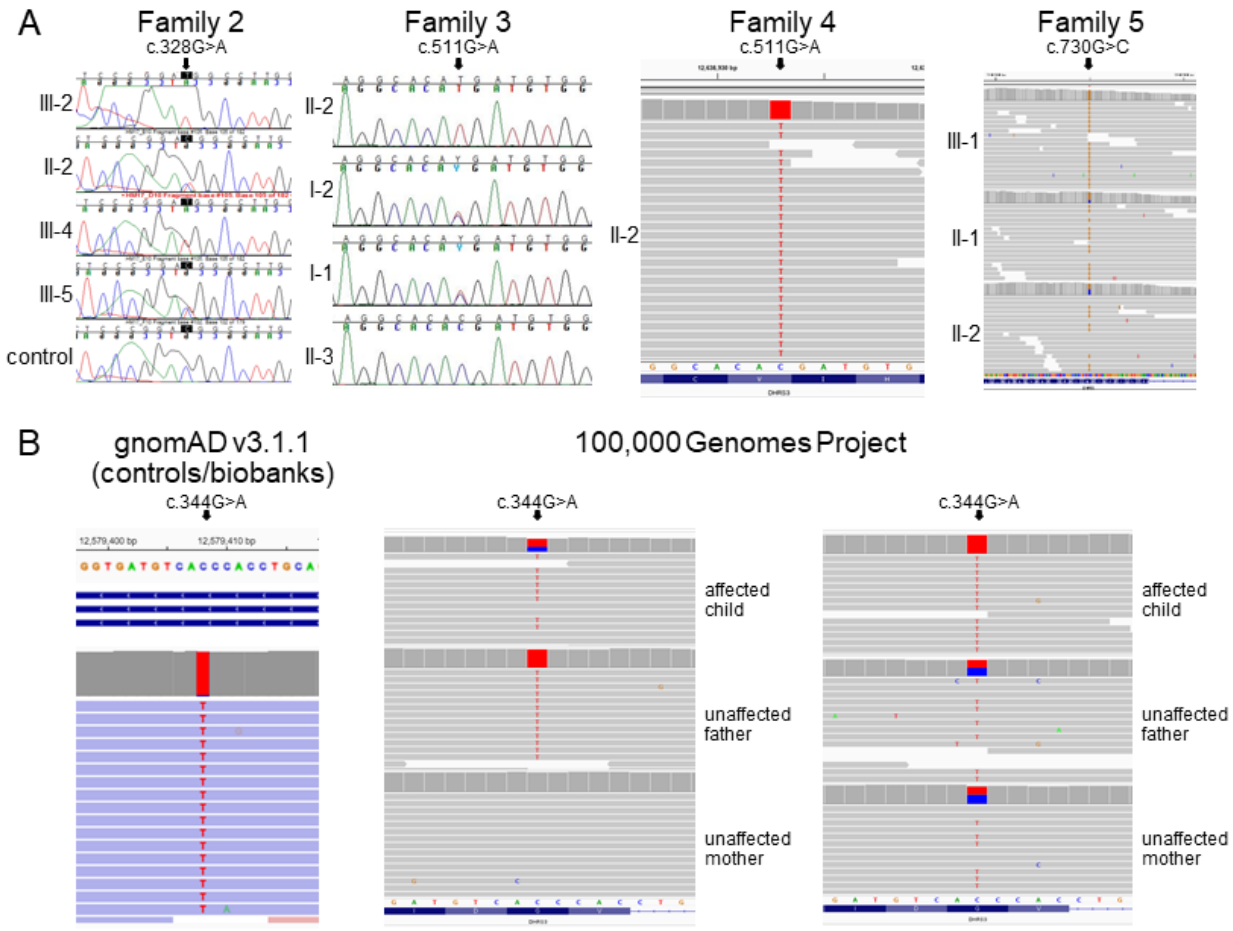

Supplemental Fig 4. Confirmation of variants in dideoxy-sequencing traces or Integrated Genomics Viewer (IGV) analysis.

A, variants present in Families 2-5. B, three independently identified homozygous c.344G>A variants. Note that the reference sequences are given for the plus strand, whereas *DHRS3* is encoded from the minus strand.

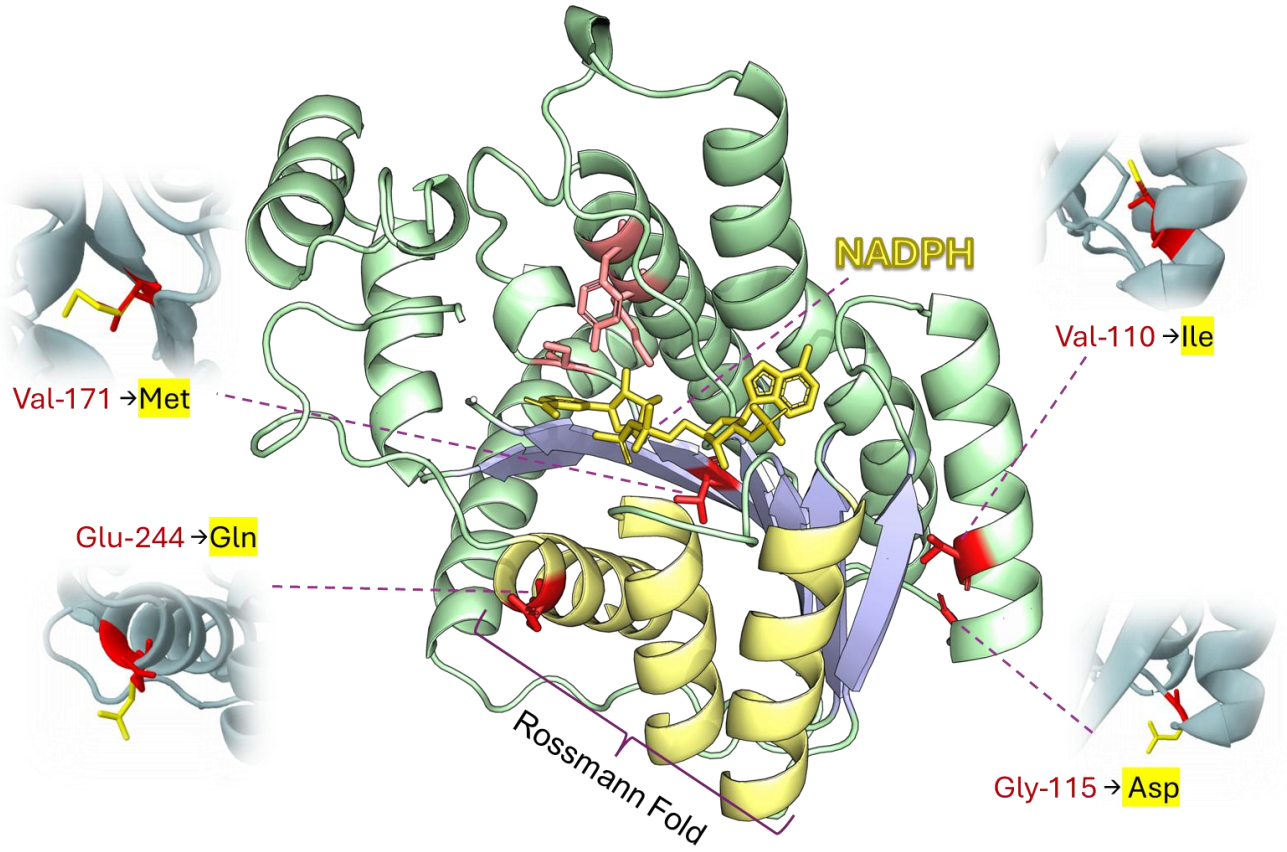

Supplemental Fig 5. Predicted structural consequences of DHRS3 missense variants.

The AlphaFold 3 prediction[31] of human DHRS3 (O75911) bound to NADPH is represented using the molecular graphics package PyMol version 3.0.0 (Schrödinger, LLC, New York, NY, USA). The DHRS3 protein backbone is colored pale green with the exception of the Rossman fold represented by seven β-sheets (light blue) and three α-helices (pale yellow). The bound NADPH cofactor is colored yellow, while p.Ser175, p.Tyr188 and p.Lys192 involved in catalysis[32] are colored pink. The side chains of the p.Val110, p.Gly115, p.Val171 and p.Glu244 residues which are substituted in the different variants are colored red. The structural prediction has very high per-atom confidence estimate based on a Local Distance Difference Test (pLDDT>90). The predicted template modeling (pTM) score and the interface predicted template modeling (ipTM) scores are 0.9 and 0.95, respectively. *Insets* display the effects of these variants on the structure of DHRS3 as modeled by Missense3d.[33] The side chains of wild-type and mutant residues are colored red and yellow, respectively.

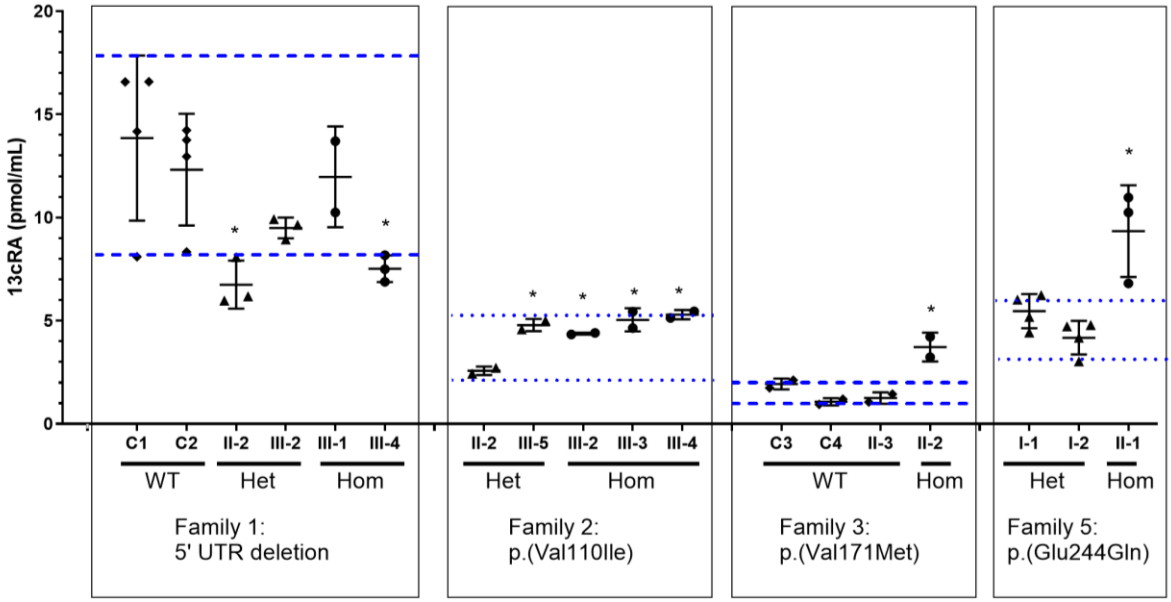

Supplemental Fig 6. Measurement of 13-cis retinoic acid (13cRA) in plasma of individuals from Families 1, 2, 3 and 5.

13cRA measurements (pmol/ml) for each set of family samples were determined by LC-MS/MS. The *x*-axis labels indicate the identity of the individual analysed (see pedigrees in Supplemental Fig 1), and below, whether they are wild-type (WT), heterozygous (Het), or homozygous (Hom) for the corresponding *DHRS3* variant. Additional unrelated wild-type controls C1-C4 were included in the analyses of Families 1 and 3. Limits for excess or deficiency displayed were calculated for each family as a subpopulation using the average WT (dashed lines) or average Het (dotted lines) levels and the critical difference from Soderlund et al..[7] Significance of differences of Hom cases within individual families, compared to unaffected individuals, were determined by one-way ANOVA with Tukey's correction for multiple comparisons. *p<0.05, **p<0.01, ***P<0.001, ****P<0.0001.

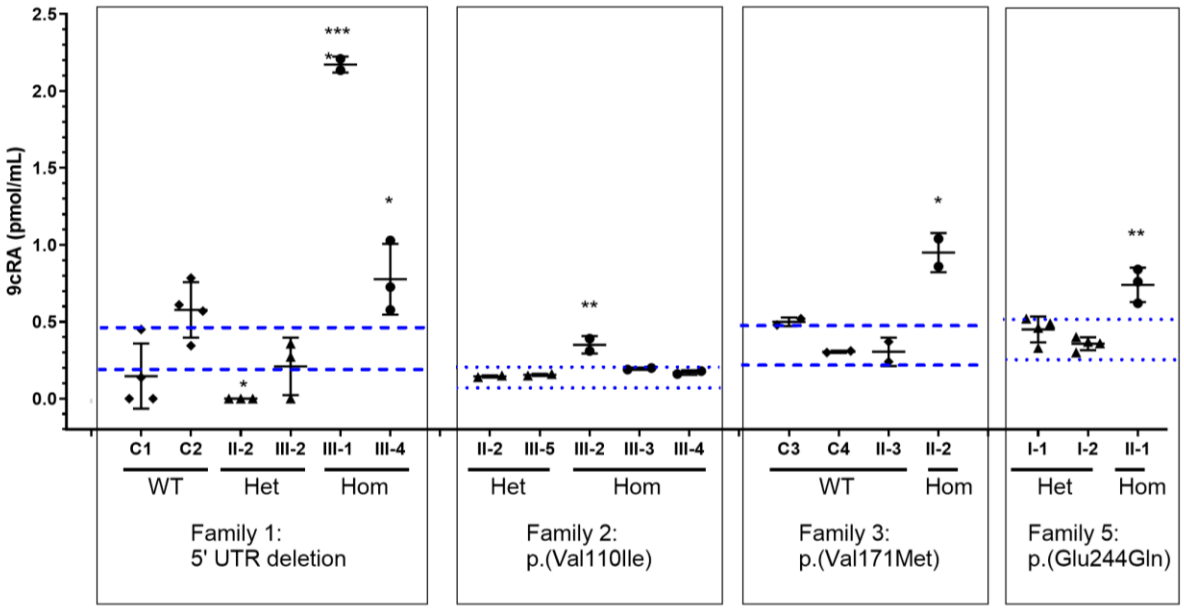

Supplemental Fig 7. Measurement of 9-cis retinoic acid (9cRA) in plasma of individuals from Families 1, 2, 3 and 5.

9cRA measurements (pmol/ml) for each set of family samples were determined by LC-MS/MS. The *x*-axis labels indicate the identity of the individual analysed (see pedigrees in Supplemental Fig 1), and below, whether they are wild-type (WT), heterozygous (Het), or homozygous (Hom) for the corresponding *DHRS3* variant. Additional unrelated wild-type controls C1-C4 were included in the analyses of Families 1 and 3. Limits for excess or deficiency displayed were calculated for each family as a subpopulation using the average WT (dashed lines) or average Het (dotted lines) levels and the critical difference from Soderlund et al..[7] Significance of differences of Hom cases within individual families, compared to unaffected individuals, were determined by one-way ANOVA with Tukey's correction for multiple comparisons. *p<0.05, **p<0.01, ***P<0.001, ****P<0.0001.

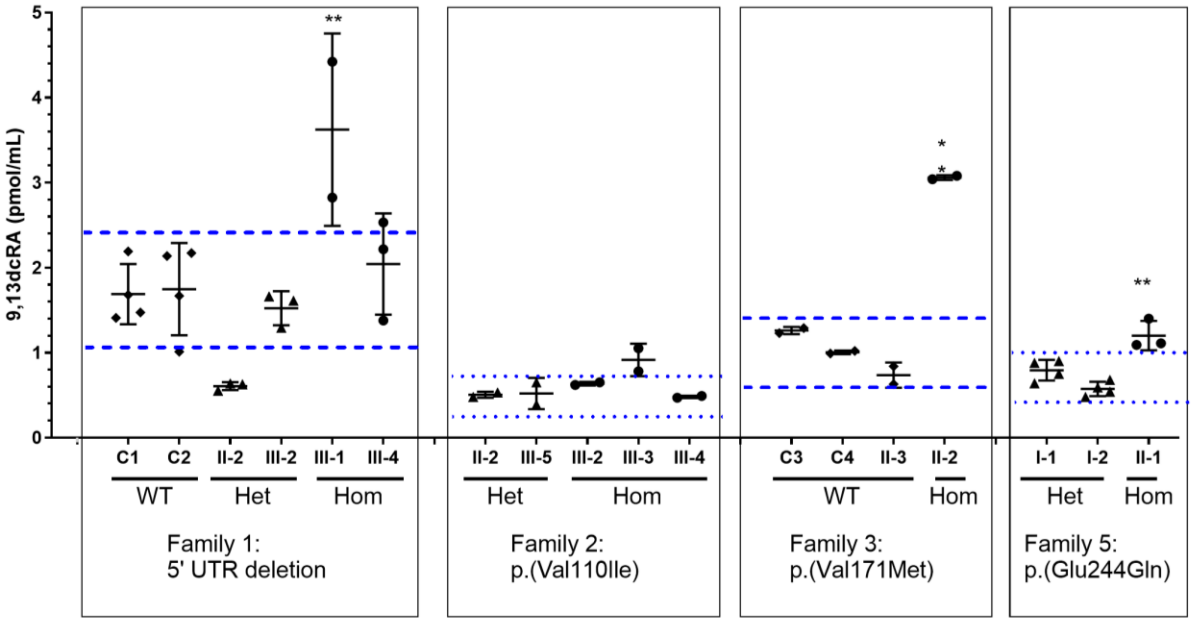

Supplemental Fig 8. Measurement of 9,13-di-cis retinoic acid (9,13dcRA) in plasma of individuals from Families 1, 2, 3 and 5.

9, 13dcRA measurements (pmol/ml) for each set of family samples were determined by LC-MS/MS. The *x*-axis labels indicate the identity of the individual analysed (see pedigrees in Supplemental Fig 1), and below, whether they are wild-type (WT), heterozygous (Het), or homozygous (Hom) for the corresponding *DHRS3* variant. Additional unrelated wild-type controls C1-C4 were included in the analyses of Families 1 and 3. Limits for excess or deficiency displayed were calculated for each family as a subpopulation using the average WT (dashed lines) or average Het (dotted lines) levels and the critical difference from Soderlund et al..[7] Significance of differences of Hom cases within individual families, compared to unaffected individuals, were determined by one-way ANOVA with Tukey's correction for multiple comparisons. *p<0.05, **p<0.01, ***P<0.001, ****P<0.0001.

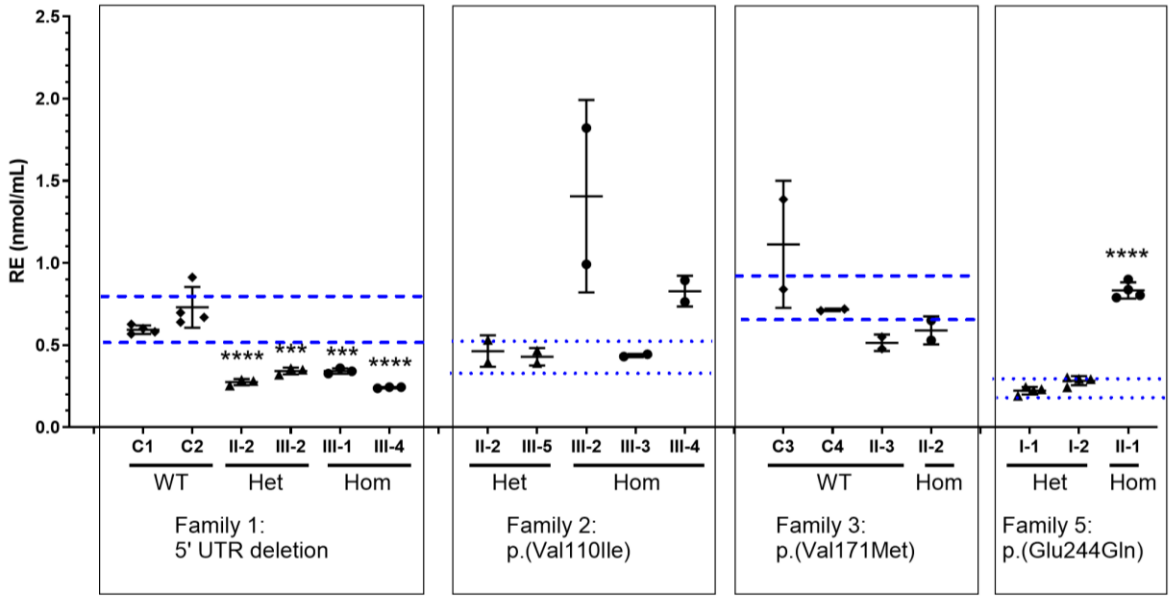

Supplemental Fig 9. Measurement of retinyl ester (RE) in plasma of individuals from Families 1, 2, 3 and 5.

Non-fasting RE measurements (nmol/ml) for each set of family samples were determined by HPLC-UV. The *x*-axis labels indicate the identity of the individual analysed (see pedigrees in Supplemental Fig 1), and below, whether they are wild-type (WT), heterozygous (Het), or homozygous (Hom) for the corresponding *DHRS3* variant. Additional unrelated wild-type controls C1-C4 were included in the analyses of Families 1 and 3. Limits for excess or deficiency displayed were calculated for each family as a subpopulation using the average WT (dashed lines) or average Het (dotted lines) levels and the critical difference for ROL as a surrogate from Soderlund et al..[7] Significance of differences of Hom cases within individual families, compared to unaffected individuals, were determined by one-way ANOVA with Tukey's correction for multiple comparisons. *p<0.05, **p<0.01, ***P<0.001, ****P<0.0001. See the accompanying text commentary for a discussion of the limitations of measuring RE in the non-fasting state.

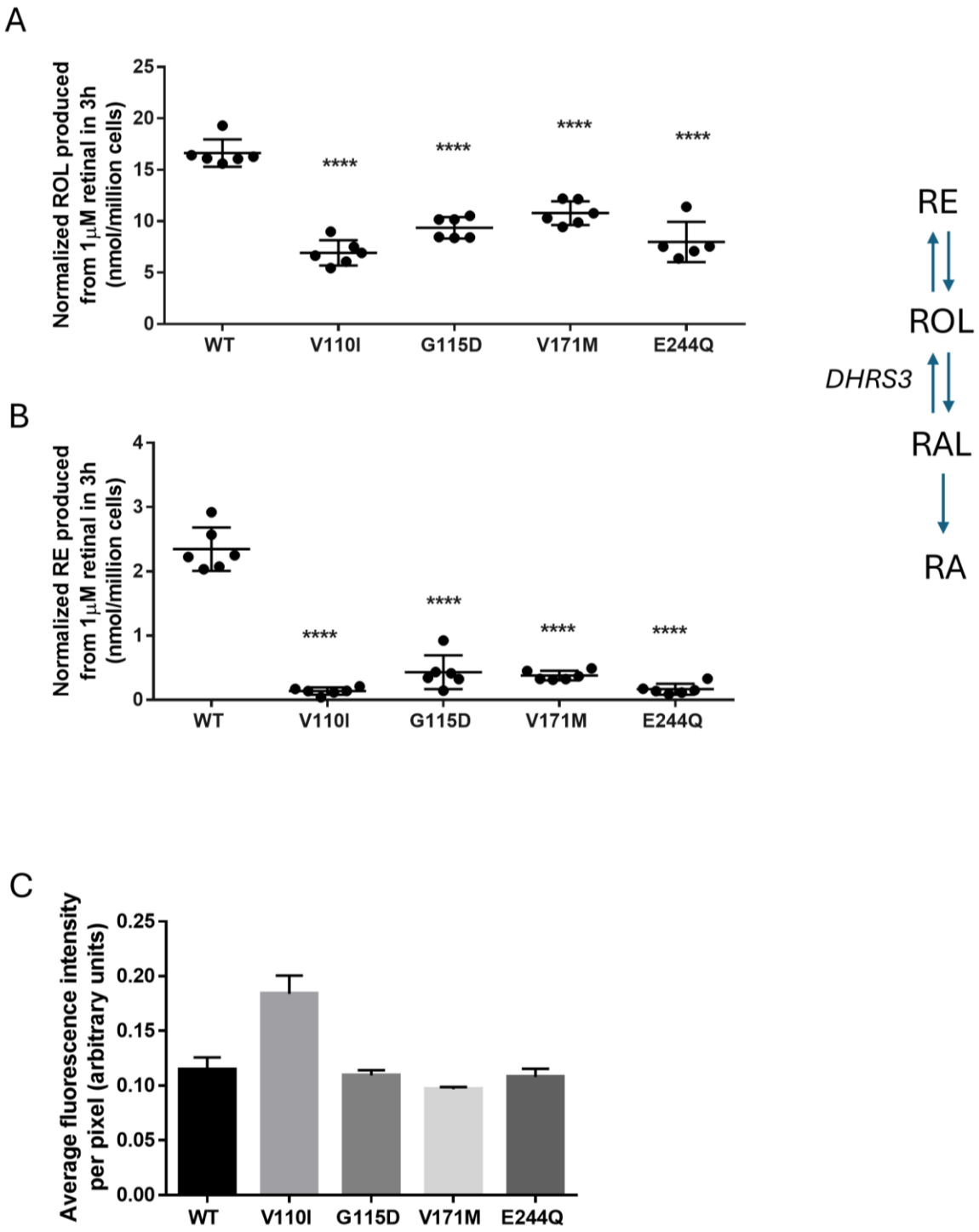

Supplemental Fig 10. In vitro measurement of DHRS3 activity via ROL and RE measurement.

Stably transfected cell lines with the variants p.Val110Ile (V110I), p.Gly115Asp (G115D), p.Val171Met (V171M), p.Glu244Gln (E244Q), or WT construct, were treated with 1 µM RAL for 3 hours and assayed for (A) ROL and (B) RE production to assess the DHRS3 loss of function. Measured retinoid levels were normalized to the average GFP fluorescence per pixel (C) to account for variations in DHRS3 expression. All variants displayed decreased ROL and decreased RE indicating a loss of DHRS3 activity. Significance of the change in activity was determined via two-tailed, unpaired t-test as compared to WT. n=5-6, independent biological replicates; ****P<0.0001. These data accompany Figure 6 of the main report, in which DHRS3 activity was evaluated via quantification of RA, and the *DHRS3* mutant lines yielded higher RA levels indicating reduced DHRS3 activity.

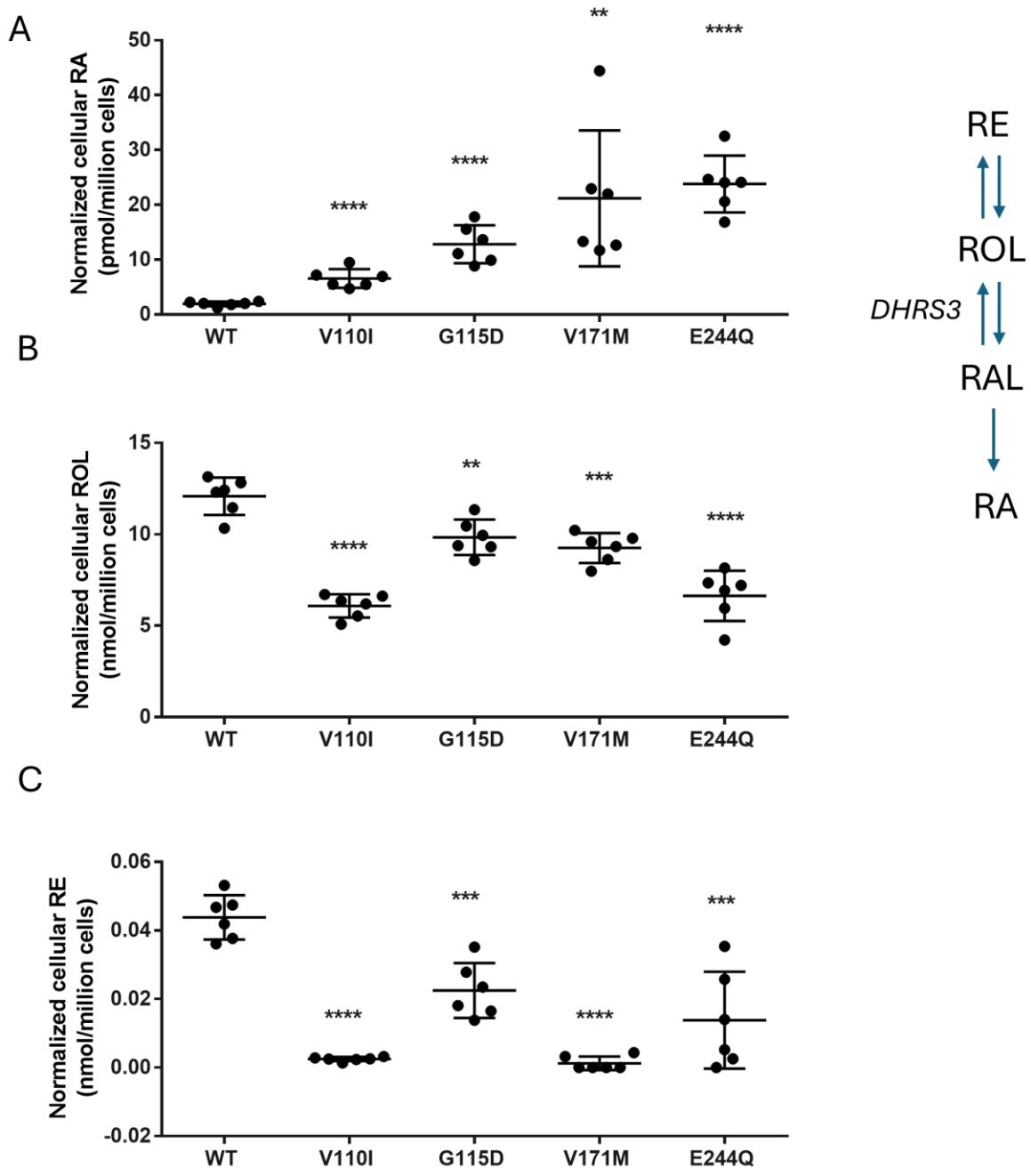

Supplemental Fig 11. Basal cellular retinoids in cell lines stably transfected with mutant DHRS3.

Stably transfected cell lines with the variants p.Val110Ile (V110I), p.Gly115Asp (G115D), p.Val171Met (V171M), p.Glu244Gln (E244Q),or WT construct, were treated with vehicle control and assayed for cellular (A) ROL, (B) RA, and (C) RE to assess the DHRS3 loss of function on basal cellular retinoids. Measured retinoid levels were normalized to the average GFP fluorescence per pixel to account for variations in DHRS3 expression (Supplemental Fig S10C). All variants displayed increased RA and decreased ROL and RE indicating a loss of DHRS3 activity. Significance of the change in activity was determined via two-tailed, unpaired t-test compared to WT. n=5-6 independent biological replicates; **P<0.01, ***P<0.001, ****P<0.0001.

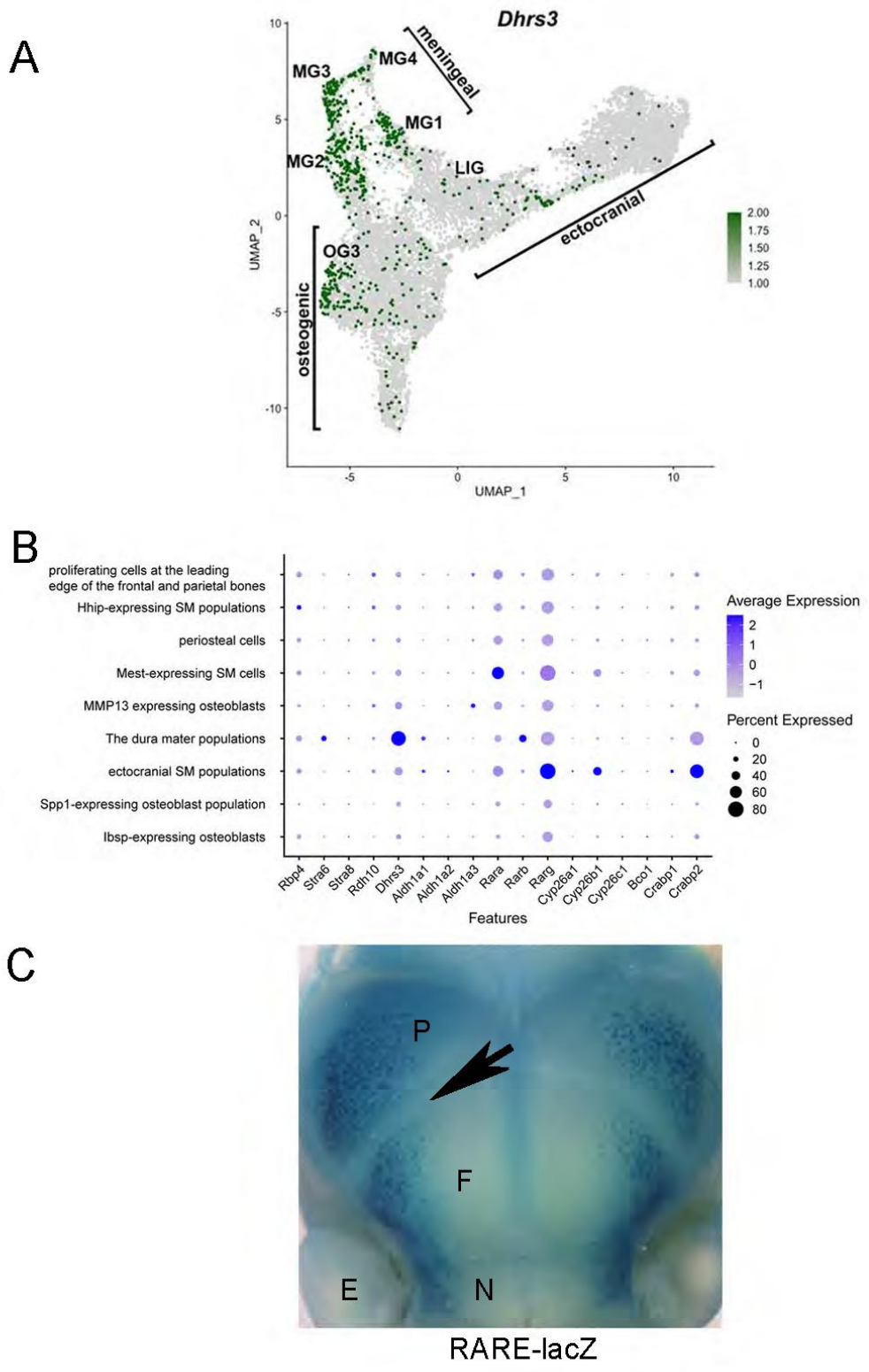

Supplemental Fig 12. Evidence for *Dhrs3* expression and retinoic acid signaling in murine skull.

A, Uniform manifold approximation and projection (UMAP) plot of *Dhrs3* expression in osteogenic/mesenchymal cell subsets, based on integrated analysis of single cell RNA sequencing data from E15.5 and E17.5 coronal sutures.[34] *Dhrs3* expression is prominent in all four meningeal clusters (MG1-MG4) and one of the four osteogenic clusters (OG3), with relatively lower expression in other cell types (ectocranial, ligament-like (LIG), and proliferative osteogenic clusters). B, Dot plot analysis of key genes

involved in vitamin A transport, retinoic acid synthesis, catabolism and signaling, in the coronal suture, based on analyses of an independent single cell RNA sequencing dataset.[35] *Dhrs3* is highly and predominantly expressed in the dura mater, osteoblast and ectocranial populations. C, Xgal (blue) staining of E18.5 *RARE-lacZ* mouse skull demonstrating the spatial pattern of retinoic acid signaling in the frontal and parietal bones on either side of the coronal sutures (arrow). Abbreviations: E, eye; F, frontal bone; N, nasal bone; P, parietal bone.

Supplemental Table 1. Experimental details for exome and genome sequencing in Families 1-5.

Individual	Study focus	Design	Library kit	Platform	Analysis software			Mean exon coverage	Filtering	Control population[a]
					Mapping	Variant calling	Annotation			
III-4, family 1	Craniosynostosis research	Exome	Illumina TruSeq V2	Illumina HiSeq 2000	Bowtie2	SAMtools v.1.1 Platypus v0.5.2	ANNOVAR	15	AF<0.005	ESP, 1000G
III-1, Family 1	Craniosynostosis research	Genome	na	Illumina HiSeq 2500	Bowtie2	SAMtools v.1.1 Platypus v0.5.2	ANNOVAR	35	AF<0.005	ESP, 1000G
II-2, Family 2	Intellectual disability in consanguineous families	Exome	Roche SeqCap EZ Exome v3.0	Illumina HiSeq 2500	BWA-0.5.10	GATK-1.6-11	SnpEff-3.3	na	AF≤0.01	See ref. 2
II-2, Family 3	Clinical diagnosis	Exome	Kit xGen Exome Panel v2.1 (IDT)	Illumina NovaSeq 600	BWA-MEM (GRCh37) 0.7.17	GATK-4.1.7.0	ANNOVAR	125	AF<0.01	gnomAD v2.1 + In-house dataset
II-1 and II-2, Family 4	Clinical diagnosis	Exome	Nextera Rapid Capture Exome v1.2	Illumina Next-Seq	BWA (GRCh37)	GATK	IAS v3	204	AF<0.01	gnomAD v2.1
III-1, Family 5	Clinical diagnosis	Trio Exome	Twist Core Exome RefSeq	Illumina NovaSeq 6000	Varfeed (from Limbus, Rostock), based on BWA	Varfeed (from Limbus, Rostock), based on GATK	Varvis (from Limbus, Rostock)	120	AF<0.01	gnomAD v2.1

[a]ESP, Exome Sequencing Project; 1000G, 1000 Genomes Project. na, not available.

Supplemental Table 2. Primers used to analyze *DHRS3* in Family 1 and the craniosynostosis patient cohort.

Purpose	**Target**	**Primer sequence 5'→3'**		**Size (bp)**	**Multiplex pool[a]**
		Forward	Reverse		
Multiplex analysis of Family 1 for 3,926 bp deletion	Deleted allele	CTGTAGAGGGAACATCACCAGCG (F)	TGAGTACCAATGGCCTCCTCACT (R1)	4431 or 505	na
	Normal allele		CCCCTCCCTAAACTCCTCTGTCA (R2)	412	na
Real time RT-PCR of *DHRS3* in Family 1	*DHRS3*	GAGATGTTCCAGGGCATGAG	TGCACAGCTTCCACTGTC	92	
	HPRT1	GACCAGTCAACAGGGGACAT	GTCAAGGGCATATCCTACAAC	261	
	ACTB	CCATGTACGTTGCTATCCAGG	CTCCTTAATGTCACGCACGAT	251	
Screen for 3,926 bp deletion[b]	Deleted allele	CAGCCGTTTCCACACCATC	CAGAGATTCCATCACATCTGCCT	388	na
Screen for variants in *DHRS3* in craniosynostosis cohort[b]	Exon 1-1	TCCTAAGGTTGGGACGGTAAA	CAATGAGTCGGGAGACTTTCG	367	C
	Exon 1-2	CAGTCCGACGGCTGCTTTCA	TAGAACTTTCCACCTCCGGCTTCC	362	A
	Exon 1-3	TGAAACCGACTAGCTCAGCACTC	CTGGTGATGTTCCCTCTACAGATGA	323	B
	Exon 2	AATCAACCCTAATCCCTGCCTATGT	GCATCACTGTGGCTTAATGACCATT	382	B
	Exon 3	TTCGTGGACATCCCTGCTGG	AAACATATATCGTTGGCCCTGGG	299	B
	Exon 4	CAGGTGAGAAGGCTGGTCT	CCCTAGAGCATCATGTGTGTC	389	C
	Exon 5	CAAATGTGCCAGCACTCCTC	CCAAAGGGTGACCCAGACAT	324	C
	Exon 6	CTCACCCAGCAGAAGCATG	GGAGCACTTTCAGGAACCAG	303	A

[a]Pooling used for multiplex PCR of amplicions as described in Supplemental Methods (Screen for *DHRS3* variants in the craniosynostosis cohort.)

[b]CS1 and CS2-tags were added to the start of the forward and reverse primers respectively, see Supplemental Methods.

Supplemental Table 3. Genotyping of rare homozygous nonsynonymous variants shared by affected individuals (III-1 and III-4) in Family 1.

Gene	Position (GRCh37)	Nucleotide change (MANE Select except *)	Amino acid change	Frequency (ExAC)	Genotype by dideoxy-sequencing				
					II-1	II-2	III-4	III-1	III-2
PLOD1	NC_000001.10:g.12012748G>A	NM_000302.4:c.535G>A	p.D179N	0.0005366	AG	AG	AA	AA	AA
SEC23IP	NC_000010.10:g.121658469C>T	NM_007190.4:c.694C>T	p.P232S	0.0004230	AT	AT	TT	TT	TT
PKM	NC_000015.9:g.72511424A>G	*NM_001206798.3:c.62T>C	p.I21T	0.0006515	CT	CT	CC	CC	CC
NEO1	NC_000015.9:g.73575321T>G	NM_002499.4:c.3279T>G	p.H1093Q	0.0006263	GT	GT	GG	GG	GG

Supplemental Table 4. Analysis of probe dropouts from SNP array analysis of III-1 in Family 1

Position (GRCh38)	Length (bp)	Number of probes	Genes in region	Filtering				
				Homozygous regions of		Verified in GS of III-1	Similar CNVs in DGV	Additional information (distance to genes, conservation and regulatory signals in ENCODE)
				III-1	III-4			
chr1:8295859-8306027	10169	10	*SLC45A1*	Y	Y	Y	Y	intergenic, 16 kb away from *SLC45A1*, conserved down to zebrafish
chr1:12618127-12623043	4917	10	*DHRS3*	Y	Y	Y	no exact match	5'-UTR of *DHRS3*, partially conserved down to *X.tropicalis* High H3K4Me1, H3K4Me3 and H327Ac in ENCODE
chr1:14580568-14582946	2379	1		N	N			
chr2:17574696-17575348	653	1	*VSNL1*	N	N			
chr2:55288607-55289358	752	2	*CCDC88A*	Y	N			
chr2:214780669-214780864	196	5	*BARD1*	N	N			
chr3:65132184-65132492	309	1		N	N			
chr3:194358639-194358756	118	2	*LRRC15*	Y	N			
chr3:198113116-198113277	162	2		Y	N			
chr4:92141101-92141600	500	1		Y	N			
chr5:145130840-145133264	2425	1		Y	N			
chr6:15438419-15441336	2918	2	*JARID2*	Y	N			
chr6:162379546-162379698	153	2	*PARK2*	Y	N			

chr7:156594462-156603008	8547	10	*LINC01006*	Y	N			
chr8:19093538-19093695	158	1		Y	N			
chr8:23122999-23132105	9107	10		Y	N			
chr10:77565652-77566538	887	1	*KCNMA1*	Y	N			
chr10:79790853-79851251	60399	1	*NUTM2B-AS1* *LOC642361*	Y	N			
chr11:81788506-81810088	21583	12		N	Y			
chr14:80664561-80670434	5874	8	*CEP128*	Y	N			
chr15:63338895-63339280	386	1	*CA12*	Y	Y	N		
chr16:69007782-69011396	3615	2	*TANGO6*	Y	Y	Y	no exact match	intronic, ~11.5 kb away from *TANGO6* exon 16, not conserved in mouse and other species
chr16:82974702-82976354	1653	2	*LOC1019284* *17 CDH13*	Y	Y	N		
chr18:50604720-50605268	549	1	*MAPK4*	Y	N			
chr18:62498088-62500268	2181	2		Y	N			
chr19:20417027-20534411	117385	24	*ZNF826P*	Y	N			
chr22:25054828-25056756	1929	1	*KIAA1671*	Y	N			

Supplemental Table 5. Rare homozygous variants identified in Individual II-1 in Family 5.

Gene	OMIM disease gene?	gDNA alteration (GRCh38)	cDNA alteration	Amino acid alteration	dbSNP ID	Maximum gnomAD v.2 population frequency	CADD score	REVEL score	Alpha Missense prediction
AHNAK	No	NC_000011.10:g.62522674C>T	NM_001620.3:c.11743G>A	p.(Asp3915Asn)	rs1202972883	0.00005 (East Asian)	22.3	0.157	0.128
ANK3	Intellectual developmental disorder, autosomal recessive 3	NC_000010.11:g.60076176A>C	NM_020987.5:c.4705T>G	p.(Ser1569Ala)	rs375050420	0.0001 (Latino/Admixed American)	26.0	0.324	0.145
DHRS3	No	NC_000001.11:g.12572822C>G	NM_004753.7:c.730G>C	p.(Glu244Gln)	rs1389365121	0.00001 (non-Finnish European)	22.8	0.591	0.179
MPZL2	Deafness, autosomal recessive 111	NC_000011.10:g.118262459G>A	NM_005797.4:c.415C>T	p.(Arg139Trp)	rs182816672	0.00025 (East Asian)	32	0.377	0.149
PC	Pyruvate carboxylase deficiency (autosomal recessive)	NC_000011.10:g.66871123C>T	NM_001040716.2:c.562G>A	p.(Gly188Ser)	rs770763439	0.0002 (East Asian)	25.5	0.938	0.192

Supplemental Table 6. Retinoid levels in patient plasma. Mean ± standard deviation (*n*).

			Fig 5A	Fig 5B	Fig S6	Fig S7	Fig S8	Fig S9
Family[a]	**Geno -type**	**ID**	**ROL (nmol/mL)**	**RA (pmol/mL)**	**13c-RA (pmol/mL)**	**9c-RA (pmol/mL)**	**9,13-dcRA (pmol/mL)**	**RE (nmol/mL)**
1	WT	C1	2.1 ± 0.1 (4)	10.2 ± 0.8 (4)	13.9 ± 4.0 (4)	0.1 ± 0.2 (4)	1.7 ± 0.4 (4)	0.6 ± 0.02 (4)
1	WT	C2	2.6 ± 0.1 (4)	10.1 ± 0.7 (4)	12.3 ± 2.7 (4)	0.6 ± 0.2 (4)	1.7 ± 0.5 (4)	0.7 ± 0.1 (4)
1	Het	II-2	1.1 ± 0.03 (3)	12.1 ± 0.5 (3)	6.8 ± 1.2 (3)	n.d. ± (3)	0.6 ± 0.05 (3)	0.3 ± 0.02 (3)
1	Het	III-2	1.5 ± 0.2 (3)	11.6 ± 0.9 (3)	9.5 ± 0.5 (3)	0.2 ± 0.2 (3)	1.5 ± 0.2 (3)	0.3 ± 0.02 (3)
1	Hom	III-1	0.3 ± 0.01 (3)	18.0 ± 0.7 (3)	12.0 ± 2.4 (3)	2.2 ± 0.1 (3)	3.6 ± 1.1 (3)	0.3 ± 0.02 (3)
1	Hom	III-4	0.9 ± 0.08 (3)	16.8 ± 1.9 (2)	7.5 ± 0.6 (3)	0.8 ± 0.2 (3)	2.0 ± 0.6 (3)	0.2 ± 0.004 (3)
2	Het	II-2	1.0 ± 0.004 (2)	4.3 ± 0.2 (2)	2.6 ± 0.2 (2)	0.1 ± 0.01 (2)	0.5 ± 0.03 (2)	0.5 ± 0.1 (2)
2	Het	III-5	0.8 ± 0.04 (2)	4.7 ± 0.02 (2)	4.8 ± 0.3 (2)	0.2 ± 0.01 (2)	0.5 ± 0.2 (2)	0.4 ± 0.1 (2)
2	Hom	III-2	0.3 ± 0.04 (2)	5.8 ± 0.6 (2)	4.4 ± 0.05 (2)	0.4 ± 0.1 (2)	0.6 ± 0.02 (2)	1.4 ± 0.6 (2)
2	Hom	III-3	1.0 ± 0.04 (2)	6.6 ± 0.6 (2)	5.0 ± 0.6 (2)	0.2 ± 0.01 (2)	0.9 ± 0.2 (2)	0.4 ± 0.01 (2)
2	Hom	III-4	0.9 ± 0.05 (2)	6.5 ± 0.1 (2)	5.3 ± 0.2 (2)	0.2 ± 0.01 (2)	0.5 ± 0.01 (2)	0.8 ± 0.1 (2)
3	WT	C3	1.8 ± 0.3 (2)	7.3 ± 0.2 (2)	1.9 ± 0.3 (2)	0.5 ± 0.03 (2)	1.3 ± 0.04 (2)	1.1 ± 0.4 (2)
3	WT	C4	2.0 ± 0.1 (2)	5.7 ± 0.3 (2)	1.1 ± 0.2 (2)	0.3 ± 0.01 (2)	1.0 ± 0.02 (2)	0.7 ± 0.01 (2)
3	WT	II-3	2.2 ± 0.2 (2)	7.8 ± 1.0 (2)	1.3 ± 0.3 (2)	0.3 ± 0.1 (2)	0.7 ± 0.2 (2)	0.5 ± 0.05 (2)
3	Hom	II-2	1.0 ± 0.04 (2)	17.4 ± 1.9 (2)	3.7 ± 0.7 (2)	1.0 ± 0.1 (2)	3.1 ± 0.03 (2)	0.6 ± 0.1 (2)
5	Het	I-1	2.1 ± 0.2 (4)	5.2 ± 0.3 (4)	5.5 ± 0.8 (4)	0.5 ± 0.1 (4)	0.8 ± 0.1 (4)	0.2 ± 0.02 (4)
5	Het	I-2	1.2 ± 0.1 (4)	5.6 ± 0.3 (4)	4.2 ± 0.8 (4)	0.4 ± 0.04 (4)	0.6 ± 0.1 (4)	0.3 ± 0.03 (4)
5	Hom	II-1	1.3 ± 0.1 (4)	11.0 ± 0.2 (3)	9.3 ± 2.2 (3)	0.7 ± 0.01 (3)	1.2 ± 0.2 (3)	0.8 ± 0.05 (4)

[a]Family 1: 5'-UTR deletion; Family 2: p.(Val110Ile), Family 3: p.(Val171Met), Family 5: p.(Glu244Gln)

Supplemental Table 7: Calculated limits for excess or deficiency[a].

			Fig 5	Fig S6	Fig S7	Fig S8	Fig S5	Fig S9
Family	**Genotype**	**control group**	**RA (pmol/mL)**	**13c-RA (pmol/mL)**	**9c-RA (pmol/mL)[b]**	**9,13-dcRA (pmol/mL)[b]**	**ROL (nmol/mL)**	**RE (nmol/mL)[c]**
1	5'-UTR deletion	WT	6.3 – 14.0	8.2 – 17.9	0.22 – 0.50	1.1 – 2.4	1.9 – 2.8	0.54 – 0.78
2	p.(Val110Ile)	Het	2.8 – 6.2	2.3 – 5.0	0.09 – 0.21	0.32 – 0.71	0.7 – 1.0	0.37 – 0.53
3	p.(Val171Met)	WT	4.3 – 9.5	0.9 – 1.9	0.23 – 0.51	0.62 – 1.4	1.6 – 2.3	0.64 – 0.92
5	p.(Glu244Gln)	Het	3.3 – 7.5	3.0 – 6.6	0.25 – 0.56	0.42 – 0.94	1.4 – 2.0	0.21 – 0.30

[a]Subpopulation limits for excess or deficiency were calculated using the average control group level and the critical difference at the 95% confidence level as in Soderlund et al.[7]

Index of individuality (Ii): RA = 0.86, 13c-RA = 0.6, ROL = 0.27

Critical differences at 95% confidence level: RA = 38%, 13c-RA = 37%, ROL = 18%.

[b]9c-RA and 9,13dc-RA did not have literature values for Ii or critical difference, so values for RA were used as a surrogate.

[c]RE levels are not from the fasted state and have a variable post-prandial effect, so no interpretation in regard to genotype should be made. However, for illustrative purposes, the critical difference for ROL was used as a surrogate to indicate likely limits.

Supplemental References

1. Sobreira, N., Schiettecatte, F., Valle, D., and Hamosh, A. (2015). GeneMatcher: a matching tool for connecting investigators with an interest in the same gene. Hum Mutat *36*, 928-930.
2. Froukh, T.J. (2017). Next Generation Sequencing and Genome-Wide Genotyping Identify the Genetic Causes of Intellectual Disability in Ten Consanguineous Families from Jordan. Tohoku J Exp Med *243*, 297-309.
3. Koelling, N., Bernkopf, M., Calpena, E., Maher, G.J., Miller, K.A., Ralph, H.K., Goriely, A., and Wilkie, A.O.M. (2019). amplimap: a versatile tool to process and analyze targeted NGS data. Bioinformatics *35*, 5349-5350.
4. Thorvaldsdottir, H., Robinson, J.T., and Mesirov, J.P. (2013). Integrative Genomics Viewer (IGV): high-performance genomics data visualization and exploration. Brief Bioinform *14*, 178-192.
5. Harris, E.K. (1974). Effects of intra- and interindividual variation on the appropriate use of normal ranges. Clin Chem *20*, 1535-1542.
6. Petersen, P.H., Fraser, C.G., Sandberg, S., and Goldschmidt, H. (1999). The index of individuality is often a misinterpreted quantity characteristic. Clin Chem Lab Med *37*, 655-661.
7. Soderlund, M.B., Sjoberg, A., Svard, G., Fex, G., and Nilsson-Ehle, P. (2002). Biological variation of retinoids in man. Scand J Clin Lab Invest *62*, 511-519.
8. Murphy, E.A. and Abbey, H. (1967). The normal range--a common misuse. J Chronic Dis *20*, 79-88.
9. Obrochta, K.M., Kane, M.A., and Napoli, J.L. (2014). Effects of diet and strain on mouse serum and tissue retinoid concentrations. PLoS One *9*, e99435.
10. Eckhoff, C., Bailey, J.R., Collins, M.D., Slikker, W., Jr., and Nau, H. (1991). Influence of dose and pharmaceutical formulation of vitamin A on plasma levels of retinyl esters and retinol and metabolic generation of retinoic acid compounds and beta-glucuronides in the cynomolgus monkey. Toxicol Appl Pharmacol *111*, 116-127.
11. Talwar, D.K., Azharuddin, M.K., Williamson, C., Teoh, Y.P., McMillan, D.C., and O'Reilly, D.St.J. (2005). Biological variation of vitamins in blood of healthy individuals. Clin Chem *51*, 2145-2150.
12. Nagy, A. (2003). Manipulating the Mouse Embryo: A Laboratory Manual. Cold Spring Harbor, NY, USA Cold Spring Harbor Laboratory Press.
13. Rossant, J., Zirngibl, R., Cado, D., Shago, M., and Giguere, V. (1991). Expression of a retinoic acid response element-hsplacZ transgene defines specific domains of transcriptional activity during mouse embryogenesis. Genes Dev *5*, 1333-1344.
14. West, K.P., Jr. (2002). Extent of vitamin A deficiency among preschool children and women of reproductive age. J Nutr *132*, 2857S-2866S.
15. Kane, M.A. and Napoli, J.L. (2010). Quantification of endogenous retinoids. Methods Mol Biol *652*, 1-54.
16. Arnhold, T., Tzimas, G., Wittfoht, W., Plonait, S., and Nau, H. (1996). Identification of 9-cis-retinoic acid, 9,13-di-cis-retinoic acid, and 14-hydroxy-4,14-retro-retinol in human plasma after liver consumption. Life Sci *59*, PL169-177.
17. Arnold, S.L.M., Amory, J.K., Walsh, T.J., and Isoherranen, N. (2012). A sensitive and specific method for measurement of multiple retinoids in human serum with UHPLC-MS/MS. J Lipid Res *53*, 587-598.
18. Jones, J.W., Pierzchalski, K., Yu, J., and Kane, M.A. (2015). Use of fast HPLC multiple reaction monitoring cubed for endogenous retinoic acid quantification in complex matrices. Anal Chem *87*, 3222-3230.
19. Kane, M.A., Folias, A.E., Wang, C., and Napoli, J.L. (2008). Quantitative profiling of endogenous retinoic acid in vivo and in vitro by tandem mass spectrometry. Anal Chem *80*, 1702-1708.
20. Kane, M.A., Chen, N., Sparks, S., and Napoli, J.L. (2005). Quantification of endogenous retinoic acid in limited biological samples by LC/MS/MS. Biochem J *388*, 363-369.
21. Kane, M.A., Folias, A.E., and Napoli, J.L. (2008). HPLC/UV quantitation of retinal, retinol, and retinyl esters in serum and tissues. Anal Biochem *378*, 71-79.
22. Eckhoff, C., Collins, M.D., and Nau, H. (1991). Human plasma all-trans-, 13-cis- and 13-cis-4-oxoretinoic acid profiles during subchronic vitamin A supplementation: comparison to retinol and retinyl ester plasma levels. J Nutr *121*, 1016-1025.
23. Kraft, J.C. and Juchau, M.R. (1993). 9-cis-retinoic acid: a direct-acting dysmorphogen. Biochem

Pharmacol *46*, 709-716.
24. Thaller, C., Hofmann, C., and Eichele, G. (1993). 9-cis-retinoic acid, a potent inducer of digit pattern duplications in the chick wing bud. Development *118*, 957-965.
25. Krasinski, S.D., Russell, R.M., Otradovec, C.L., Sadowski, J.A., Hartz, S.C., Jacob, R.A., and McGandy, R.B. (1989). Relationship of vitamin A and vitamin E intake to fasting plasma retinol, retinol-binding protein, retinyl esters, carotene, alpha-tocopherol, and cholesterol among elderly people and young adults: increased plasma retinyl esters among vitamin A-supplement users. Am J Clin Nutr *49*, 112-120.
26. Krasinski, S.D., Cohn, J.S., Schaefer, E.J., and Russell, R.M. (1990). Postprandial plasma retinyl ester response is greater in older subjects compared with younger subjects. Evidence for delayed plasma clearance of intestinal lipoproteins. J Clin Invest *85*, 883-892.
27. Tanumihardjo, S.A., Russell, R.M., Stephensen, C.B., Gannon, B.M., Craft, N.E., Haskell, M.J., Lietz, G., Schulze, K., and Raiten, D.J. (2016). Biomarkers of Nutrition for Development (BOND)-Vitamin A Review. J Nutr *146*, 1816S-1848S.
28. Krasinski, S.D., Cohn, J.S., Russell, R.M., and Schaefer, E.J. (1990). Postprandial plasma vitamin A metabolism in humans: a reassessment of the use of plasma retinyl esters as markers for intestinally derived chylomicrons and their remnants. Metabolism *39*, 357-365.
29. Relas, H., Gylling, H., and Miettinen, T.A. (2000). Effect of stanol ester on postabsorptive squalene and retinyl palmitate. Metabolism *49*, 473-478.
30. Stein, L.D., Mungall, C., Shu, S., Caudy, M., Mangone, M., Day, A., Nickerson, E., Stajich, J.E., Harris, T.W., Arva, A., et al. (2002). The generic genome browser: a building block for a model organism system database. Genome Res *12*, 1599-1610.
31. Abramson, J., Adler, J., Dunger, J., Evans, R., Green, T., Pritzel, A., Ronneberger, O., Willmore, L., Ballard, A.J., Bambrick, J., et al. (2024). Accurate structure prediction of biomolecular interactions with AlphaFold 3. Nature *630*, 493-500.
32. Haeseleer, F., Huang, J., Lebioda, L., Saari, J.C., and Palczewski, K. (1998). Molecular characterization of a novel short-chain dehydrogenase/reductase that reduces all-trans-retinal. J Biol Chem *273*, 21790-21799.
33. Ittisoponpisan, S., Islam, S.A., Khanna, T., Alhuzimi, E., David, A., and Sternberg, M.J.E. (2019). Can Predicted Protein 3D Structures Provide Reliable Insights into whether Missense Variants Are Disease Associated? J Mol Biol *431*, 2197-2212.
34. Farmer, D.T., Mlcochova, H., Zhou, Y., Koelling, N., Wang, G., Ashley, N., Bugacov, H., Chen, H.J., Parvez, R., Tseng, K.C., et al. (2021). The developing mouse coronal suture at single-cell resolution. Nat Commun *12*, 4797.
35. Holmes, G., Gonzalez-Reiche, A.S., Saturne, M., Motch Perrine, S.M., Zhou, X., Borges, A.C., Shewale, B., Richtsmeier, J.T., Zhang, B., van Bakel, H., et al. (2021). Single-cell analysis identifies a key role for Hhip in murine coronal suture development. Nat Commun *12*, 7132.